Metabolic Engineering 57 (2020) 151–161

Contents lists available at ScienceDirect

Metabolic Engineering

journal homepage: www.elsevier.com/locate/meteng

The yeast peroxisome: A dynamic storage depot and subcellular factory for squalene overproduction

Guo-Song Liu, Tian Li, Wei Zhou, Min Jiang, Xin-Yi Tao, Min Liu, Ming Zhao, Yu-Hong Ren, Bei Gao*, Feng-Qing Wang**, Dong-Zhi Wei***

State Key Laboratory of Bioreactor Engineering, Newworld Institute of Biotechnology, East China University of Science and Technology, 130 Meilong Road, Shanghai, 200237, China

ARTICLE INFO

Keywords:
Synthetic biology
Saccharomyces cerevisiae
Peroxisome
Storage depot
Subcellular factory
Terpene

ABSTRACT

Engineering microbes to produce terpenes from renewable feedstock is a promising alternative to traditional production approaches. Generally, terpenes are not readily secreted by microbial cells, and their distribution within cells is usually obscure and often a restricting factor for the overproduction of terpenes due to the storage limitation. Here, we determined that squalene overproduced in the cytoplasm of *Saccharomyces cerevisiae* was distributed in a form similar to oil droplets. Interestingly, these suspected oil droplets were confirmed to be inflated peroxisomes that were swollen along with the production of squalene, indicating that peroxisomes in *S. cerevisiae* are dynamic depots for the storage of squalene. In view of this, harnessing peroxisomes as subcellular compartments for squalene synthesis was performed, achieving a 138-fold improvement in squalene titer (1312.82 mg/L) relative to the parent strain, suggesting that the peroxisome of *S. cerevisiae* is an efficient subcellular factory for the synthesis of terpenes. By dual modulation of cytoplasmic and peroxisomal engineering, the squalene titer was further improved to 1698.02 mg/L. After optimizing a two-stage fed-batch fermentation method, the squalene titer reached 11.00 g/L, the highest ever reported. This provides new insight into the synthesis and storage of squalene in peroxisomes and reveals the potential of harnessing peroxisomes to overproduce terpenes in *S. cerevisiae* through dual cytoplasmic-peroxisomal engineering.

1. Introduction

Terpenes are the largest category of structurally diverse natural products and are derived from various living organisms including microbes, diverse plants, terraneous animals, and marine species (Li et al., 2019; Tetali, 2019). To date, more than 70,000 terpenes and terpene-derived molecules have been identified, many of which exhibit a wide variety of application value as antitumor drugs, food and cosmetic additives, fragrances, and biofuels (Bian et al., 2017; Moser and Pichler, 2019; Paramasivan and Mutturi, 2017). Engineering microbes to produce these valuable terpenes has been proposed as a promising alternative to the traditional plant extraction and chemical synthesis approaches because microbial production is low in cost, sustainable and environmentally friendly (Ye et al., 2016).

Yeasts are considered potential platforms for terpene production due to their robust growth, ease of genetic manipulation, and intrinsic mevalonate (MVA) pathway for terpene biosynthesis. Multiple engineering strategies have been implemented in microbial cells to produce terpenes, including introducing heterologous terpene synthases (Jiang et al., 2017), increasing metabolic flux (Westfall et al., 2012), and reducing the consumption of target chemicals (Naziri et al., 2011). Despite the effectiveness of these approaches in terpene biosynthesis, the intracellular distribution of terpene molecules is another challenge because the accumulation of these terpenes may be toxic to hosts (Brennan et al., 2012), and feedback inhibits the pathway, impairing the synthesis of the target products (Banerjee and Sharkey, 2014). Some small-molecule terpenes can be transferred out of the cells (Martinez et al., 2009; Walsh, 2000); however, most terpenes, especially the large molecules, always accumulate intracellularly in specific subcellular areas (Ma et al., 2019; Zhao et al., 2018). Investigation of the subcellular distribution of these large molecules is essential for understanding the mechanisms of their accumulation, transportation, and detoxification. The locations where these molecules are distributed also determine how much reserve spaces can be used for their storage,

* Corresponding author. East China University of Science and Technology, P.O.B.311, 130 Meilong Road, Shanghai, 200237, China.
** Corresponding author. East China University of Science and Technology, P.O.B.311, 130 Meilong Road, Shanghai, 200237, China.
*** Corresponding author. East China University of Science and Technology, P.O.B.311, 130 Meilong Road, Shanghai, 200237, China.
E-mail addresses: gaobei@ecust.edu.cn (B. Gao), fqwang@ecust.edu.cn (F.-Q. Wang), dzhwei@ecust.edu.cn (D.-Z. Wei).

https://doi.org/10.1016/j.ymben.2019.11.001
Received 12 September 2019; Received in revised form 19 October 2019; Accepted 5 November 2019
Available online 09 November 2019

which will directly affect their production in microbes.

Similar to triacylglycerols (TAGs) and sterol esters (SEs) in hydrophobicity, intracellularly accumulated terpenes are generally considered to be incorporated into cytoplasmic lipid droplets (LDs) (Choi et al., 2018; Ferreira et al., 2018). For example, β-carotene accumulated in *Yarrowia lipolytica* was shown to be enclosed by membrane-like structures that were most likely LDs (Larroude et al., 2018), and squalene accumulation due to variation in growth conditions or genetic manipulation could result in LDs clustering in *Saccharomyces cerevisiae* (Ta et al., 2012). Although LDs might be an available organelle for the storage of hydrophobic chemicals, it was suggested that the accumulation of squalene alone was insufficient to trigger the proliferation of LDs (Spanova et al., 2010). Additionally, in non-oleaginous hosts, such as *S. cerevisiae*, storage lipids generally accumulate at limited levels (Li et al., 2007), and thus only finite storage space can be utilized. Considering these limitations, enhanced TAG biosynthesis has been applied to facilitate the accumulation of intracellular terpenes in LDs, such as squalene and lycopene in *S. cerevisiae* (Ma et al., 2019; Wei et al., 2018), but the biosynthesis of nontarget TAGs results in a waste of carbon sources and energy. Hence, we considered whether there might be other membrane-wrapped organelles in yeast, apart from LD, that could also serve as storage compartments for hydrophobic terpenes due to their similar hydrophobicity. Peroxisomes, the primary organelles involved in cell detoxification, are speculated to be promising storage organelles for lipophilic products in yeast for the following reasons: First, peroxisomes are enclosed with a single bilayer membrane (Joshi and Cohen, 2019), which allows products to pass through expediently and separates the products from the cytosol. Second, like LDs, peroxisomes play a vital role in cellular lipid metabolism (Kohlwein et al., 2013), and the yeast peroxisome is the only site where β-oxidation of fatty acids occurs (Joshi and Cohen, 2019), which implies that peroxisomes can accommodate a certain level of hydrophobic chemicals. In addition, peroxisomes are nonessential for cell growth, and the size and number can be adjusted in response to growth conditions (Klei et al., 1997; Saraya et al., 2010).

In the peroxisomes, β-oxidation of fatty acids (Klei et al., 1997) can supply a certain amount of acetyl-CoA, which is a pivotal precursor for terpene synthesis. Moreover, a reducing redox state can be provided in the organelle by the peroxisomal NADP-dependent isocitrate dehydrogenase isoenzyme (Idp3) (Roermund et al., 2014), which can meet the NADPH requirements of terpene biosynthetic processes. Furthermore, two peptide signals for peroxisomal matrix protein targeting (Rucktaschel et al., 2011) and an enhanced C-terminal peroxisome targeting signal type 1 (ePTS1) (DeLoache et al., 2016) allow efficient introduction and localization of artificial metabolic pathways into peroxisomes. All of these traits imply that the peroxisome may be a suitable subcellular compartment for the biosynthesis of terpenes in *S. cerevisiae*.

Here, we demonstrated that the matrix of the yeast peroxisome was lipophilic by staining the yeast strain with Nile red, a dye specific for intracellular lipids. This underlined the potential of the yeast peroxisome to reserve lipophilic compounds. Specifically, the extensive lipophilic triterpene squalene synthesized in the cytoplasm of our engineered yeast strain was eventually revealed to be encapsulated into peroxisomes, the size and number of which varied with growth conditions and the accumulation of intracellular squalene. Furthermore, considering that the peroxisomal lumen is accessible to ATP, NADPH and acetyl-CoA, we compartmentalized the entire squalene synthesis pathway into peroxisomes and consequently synthesized 1312.82 mg/L squalene. Similarly, the squalene was proven to be stored in peroxisomes, indicating that the peroxisome is not only a dynamic storage depot but also a promising subcellular factory for terpene biosynthesis. In view of these advantages of peroxisomes, squalene was overproduced by taking full advantage of the productivity of the cytoplasm and peroxisomes in a hybridized yeast strain, and the highest squalene production titer ever reported (11.00 g/L) was obtained through a two-stage fed-batch fermentation. These results suggest a promising storage organelle for synthetic biology and provide a comprehensive approach for the synthesis and storage of other valuable hydrophobic chemicals.

2. Methods

2.1. Strain, media and reagents

The yeast strain used in this study was *S. cerevisiae* strain BY4741 (MATa, *his3*Δ1, *leu2*Δ0, *lys2*Δ0, *ura3*Δ0). *E. coli* DH5 (NCM Biotech, Suzhou, Jiangsu, China) was used for gene cloning. Luria-Bertani (LB) broth with antibiotics (100 μg/mL ampicillin or 50 μg/mL kanamycin) was used for cultivation of recombinant *E. coli*. YPD (1% yeast extract, 2% peptone and 2% glucose) was used for cultivation of yeast strains. SD-Leu (synthetic complete drop-out medium with 2% D-glucose and without leucine) was used for the selection of yeast strains with pTCL, a cas9 protein expression plasmid (Table S1). SD-Leu-Ura (synthetic complete drop-out medium with 2% D-glucose and without leucine and uracil) was used for the selection of yeast strains with both the pTCL and guide RNA (gRNA) plasmids. SD-Leu-FoA (SD-Leu medium with 1 mg/mL 5-fluoroorotic acid) was used for the selection of engineered yeasts with loss of the gRNA expression plasmids. Leu and Leu-Ura drop-out media were purchased from FunGenome (Beijing, China). All restriction enzymes and T4 DNA ligase were purchased from Thermo Fisher (Thermo Fisher Scientific, USA). KOD-FX DNA polymerase was purchased from TOYOBO (TOYOBO Life Science, Japan). The In-fusion Cloning Kit was purchased from NCM Biotech (NCM Biotech, Suzhou, Jiangsu, China). Antibiotics, 5-fluoroorotic acid and primers were purchased from Sangon Biotech (Shanghai, China). The standard squalene and Nile red were purchased from Sigma (Sigma Aldrich, USA).

2.2. Plasmid construction

To construct gene expression cassettes, six empty vectors (pLT 82, pLT 83, pLT 84, pLT 85, pLT 86) were first prepared (Table S1). The backbone of the six plasmids was amplified from pUC19. Promoters and terminators (Table S1) were all amplified from the genome of BY4741 and assembled by fusion PCR and In-fusion cloning. To construct cassettes of all the squalene synthesis pathway genes (*ERG10*, *ERG13*, *tHMG1*, *ERG12*, *ERG8*, *MVD1*, *IDI1*, *ERG20*, and *ERG9*), traditional restriction enzyme-based cloning was used. gRNA plasmids targeting different genome sites were designed on CRISPRdirect (http://crispr.dbcls.jp/) and constructed with PCR and In-fusion cloning. All constructed plasmids were verified by sequencing. The sequences of the primers used in this study are provided in the supplementary materials.

2.3. Yeast strain construction

All yeast strains used in this study are listed in Table 1. For the construction of each strain, the amplified upstream homologous arm, the downstream homologous arm, cassettes with no less than 50 bp overlap with the homologous arms and the gRNA plasmid were co-transformed into *S. cerevisiae* using the Frozen-EZ Yeast TransformationIITM Kit (ZYMO RESEARCH, USA) and plated on SD-Leu-Ura solid medium. Transformants were directly verified through colony PCR using KOD-FX (TOYOBO, Japan). To achieve continuous gene editing, the engineered strains were cross-streaked on an SD-Leu-5 FoA plate to remove gRNA plasmids.

2.4. Shaking flask cultivation of engineered yeasts

A total of 50 mL of YPDG medium (1% yeast extract, 2% peptone, 1% D-glucose and 1% glycerol) was used for cultivation of the engineered yeasts in a 250 mL shaking flask. To alleviate the metabolic burden, the gRNA plasmid was removed from the engineered strain

Table 1
S. cerevisiae strains used in this work.

Strain	Host strain	Description	Resource
BY4741		MATa, his3Δ1, leu2Δ0, met15Δ0, ura3Δ0	
BY47419	BY4741	pTCL	This study
BY4741G	BY47419	pGS218-GFP	This study
BY4741GE	BY47419	pGS212-GFP-ePTS1	This study
SquC1	BY47419	LPP1Δ::P_{PGK1}-ERG8, P_{TEF1}-ERG12; GAL80Δ::P_{FBA1}-ERG10, P_{HXT7}-ERG13; GAL1-7Δ::P_{HXT7}-IDI1, P_{FBA1}-MVD1; DPP1Δ::P_{PGK1}-ERG9, P_{TEF1}-ERG20; HOΔ::P_{GAL1}-tHMG1;	This study
SquC2	SquC1	HO::P_{GAL10}-NADH-HMGR	This study
SquC3	SquC2	P_{ERG1}Δ::P_{HXT1}	This study
SquC3GE	SquC3	pGS212-GFP-ePTS1	This study
SquC4	SquC3	MATaΔ::MATα	This study
SquC5	SquC4	ura3::Leu2,URA3; his3::His3; met15::Met15	This study
SquP1	BY47419	LPP1Δ::P_{PGK1}-ERG8-ePTS1, P_{TEF1}-ERG12-ePTS1; GAL80Δ::P_{FBA1}-ERG10-ePTS1, P_{HXT7}-ERG13-ePTS1; GAL1-7Δ::P_{HXT7}-IDI1-ePTS1, P_{FBA1}-MVD1-ePTS1; HOΔ::P_{GAL1}-tHMG1-ePTS1, P_{GAL10}-NADH-HMGR-ePTS1; DPP1Δ::P_{PGK1}-ERG9-ePTS1, P_{TEF1}-ERG20-ePTS1	This study
SquP2	SquP1	P_{ERG1}Δ::P_{HXT1}	This study
SquP3	SquP2	GPD1Δ,GPD2Δ	This study
SquP4	SquP3	GPD1:: P_{GAL1}-tHMG1-ePTS1, P_{GAL10}-IDI1-ePTS1	This study
SquP5	SquP4	GPD2:: P_{GAL1}-tHMG1-ePTS1, P_{GAL10}-IDI1-ePTS1	This study
SquP6	SquP5	RHR2Δ::P_{TDH3}-ANT1	This study
SquP7	SquP6	RHR2::P_{PGK1}-IDP2, P_{TEF1}-IDP3	This study
SquP8	SquP7	Cit2Δ	This study
SquP9	SquP8	Cit2::P_{PGAL1}-ACS1-ePTS1	This study
SquP10	SquP9	DPP1::P_{GAL10}-ACL1-ePTS1, P_{GAL1}-ACL2-ePTS1	This study
SquP10 GE	SquP10	pGS212-GFP-ePTS1	This study
SquP11	SquP10	ura3::Leu2, URA3; his3::His3; met15::Met15	This study
SquCP1	SquC4/ SquP10	Diploid SquC4 × SquP10	This study
SquCP2	SquC5/ SquP11	Diploid SquC5 × SquP11	This study

before cultivation. Then, the yeast was streaked on SD-Leu plates. First, a yeast monoclone was inoculated into a 5 mL of YPD tube and cultivated for 12 h. Second, to prepare seeds for fermentation, 500 μL of culture from 5 mL tube was transferred into 50 mL of YPDG medium and cultured for approximately 16 h. Finally, the seeds were inoculated into 50 mL of fresh YPDG medium at an initial OD600 of 0.15 and cultivated for 13 d.

2.5. Transmission electron microscopy (TEM)

For TEM analysis of yeast cells, precultures grown in 50 mL of YPDG medium were washed twice with PBS and preliminarily fixed with 2.5% glutaraldehyde phosphate buffer. The prefixed cells were stored at 4 °C until subsequent analysis. Cells were postfixed in 1% osmium tetroxide and dehydrated by soaking for 15 min each in increasing concentrations of ethanol (30%, 50%, 70%, 85%, 90%, 95%, and 100%) and acetone (90% and 100%). Samples were rinsed for 3 × 10 min in 100% propylene oxide and then embedded in Spurr's resin. Then, 70 nm ultrathin sections were cut and placed on copper grids and poststained for 5 min with 8% uranyl acetate in 50% ethanol and for 5 min in Reynold's lead citrate stain. Grids were viewed with a JEM-2100 transmission electron microscope (JEOL, Tokyo, Japan) operating at 120 kV.

2.6. Visualizing squalene distribution by laser scanning confocal microscopy (LSCM)

To test the peroxisome targeting capability of ePTS1, yeast cells expressing GFP and GFP-ePTS1 were cultured in 5 mL of SD-Leu-Ura medium for 48 h and washed twice with PBS. Subsequently, 2 μL preparations were directly plated on slides and observed at 488 nm with a Nikon A1R confocal laser scanning microscope (Nikon Europe, Amsterdam, The Netherlands). To visualize GFP-ePTS1 and Nile red simultaneously, precultures cultivated in 50 mL of YPDG were stained by adding Nile red solution (1 mg/mL) in acetone to the cell suspension (1/10 vol/vol) and incubated for 60 min in the dark at room temperature. Stained cells were washed with physiological saline and resuspended in potassium phosphate buffer (pH 7.4) and then directly plated on an object slide for observation with a Nikon A1R confocal laser scanning microscope at 488 nm for GFP and 561 nm for Nile red.

2.7. Nile red fluorescence intensity detection

To explore the effect of squalene concentration on the fluorescence intensity of Nile red, the following experiments were performed. First, the same amount of Nile red was dissolved in seven different concentrations (volume percentage) of a squalene/acetone mixture (Table S4). To detect the change in the maximum excitation and emission wavelengths, the fluorescence intensity of Nile red was measured in spectral scanning mode with the following settings: from 405 nm to 585 nm for excitation with steps of 5 nm and from 590 nm to 700 nm for emission with steps of 5 nm. Fluorescence intensity was detected at 561 nm of excitation and 615 nm of emission with a CYTATION3 imaging reader (Biotek, USA).

2.8. Extraction and quantification of squalene

To extract squalene, 600 μL of cultured cells and an equal volume of ethyl acetate were mixed in 2 mL microcentrifuge tubes with 1.5 g of zirconia beads (diameter of 0.5 mm) and shaken for 20 min at 60 Hz and 4 °C using a freeze grinder (Shanghai Jingxin, China). The vibrated mixture was centrifuged at 12,000 rpm for 5 min, and the upper organic phase was used for GC detection after dehydration. The GC system (Agilent 7820 A, USA) was equipped with an HP-5 column (30 m × 0.25 mm, 0.25 μm film thickness) and a flame ionization detector (FID). The oven temperature was first maintained at 90 °C for 0.5 min, followed by gradually increasing to 280 °C at a rate of 20 °C/min and holding for 10 min. Squalene was quantified using the external labeling method. All results were reported as the average of three replicates.

2.9. Mating type switch and hybridization of yeast

Mating type switch from “a” to “α” was carried out using a CRISPR/cas9-based approach (Xie et al., 2018). The sequence targeting the Ya gene was obtained from a reference (Xie et al., 2018) (Fig. S5A). Transformants that underwent successful switching were checked by colony PCR and sequencing. With regard to hybridization, two different fresh mating type strains, 100 μL each, were mixed in a 5 mL of YPD tube and cultivated for 48 h at 30 °C. Subsequently, the mixture was streaked on a YPD plate and cultivated at 30 °C. Monoclones were verified by PCR (Fig. S5B).

2.10. Fed-batch fermentation

The media used for fed-batch fermentation were composed of YPD and 0.5 g/L MgSO4. First, seed cultures were prepared by inoculating a monoclone in a 5 mL of YPD tube and grown for approximately 24 h. Second, seed cultures were subcultured by transferring 1.5 mL of the first cultures into 500 mL flasks containing 150 mL of YPD. These

cultures were grown for approximately 24 h, and then, 10% (vol/vol) of the seed cultures were inoculated into a 5 L bioreactor (Bai Lun, China) with 3 L of medium. Fermentation was carried out at 30 °C with the pH maintained at 5.2 by automatic feeding of 2.5 M NaOH. The air flow was set at 3 vvm (air volume/working volume/min), and the dissolved oxygen (dO_2) concentration was controlled at above 30% saturation by an agitation cascade (300–700 rpm). Glucose (500 g/L) was fed into the fermenter from 10 h to 40 h to achieve rapid cell growth. Ethanol was fed into the culture to substitute for glucose as the carbon source to produce squalene after 40 h of cultivation. The ethanol concentration was maintained at approximately 5 g/L by adjusting the feeding rate. Cell growth and ethanol concentration were constantly monitored during the fermentation process.

3. Results

3.1. Investigation of the lipophilic property of the yeast peroxisome

S.cerevisiae BY4741, which is generally considered a promising platform for terpene biosynthesis, was selected as the host strain. First, BY4741GE was constructed to mark peroxisomes specifically by introducing a plasmid expressing GFP with ePTS1 (Fig. 1A). In contrast to the wide distribution of green fluorescence in the strain BY4741G expressing GFP (Table 1), the small green fluorescent spots in the strain BY4741GE expressing GFP-ePTS1 demonstrated that ePTS1-tagged GFP could efficiently display peroxisomes (Fig. S1). Subsequently, to investigate the lipophilic property of peroxisomes, BY4741GE was cultured for 13 d in a 250 mL shaking flask with 50 mL of YPDG, and stained with Nile red to visualize the distribution of lipophilic compounds and LDs through LSCM analysis (Lane et al., 2015; Wei et al., 2018). As shown in Fig. 1B, the green fluorescent spots, which represented peroxisomes, overlapped with the red spots exactly. This result demonstrated that the matrix of peroxisomes was lipophilic, endowing peroxisomes with the potential to store hydrophobic compounds. Meanwhile, it was observed that the number and size of peroxisomes in BY4741GE were almost unchanged during the whole incubation period. In addition, few LDs were highlighted by Nile red, indicating the limited synthetic capability of lipids in *S. cerevisiae*.

3.2. Yeast peroxisome as a dynamic storage depot for squalene overproduced in cytoplasm

In this study, squalene was selected to explore the storage capability of peroxisomes because squalene is an endogenous and hydrophobic triterpene, and the massive accumulation of squalene requires adequate intracellular lipophilic structure (Zhao et al., 2018).

3.2.1. Construction of a yeast with high squalene output

To construct a genetically stable strain that could overproduce squalene, the whole squalene synthesis pathway was integrated into five genome loci of BY4741: *DPP1* (ChrIV 1031419–1030,550, encoding diacylglycerol pyrophosphate phosphatase), *LPP1* (ChrIV 1455866–1455,042, encoding lipid phosphate phosphatase) (Zhang et al., 2018), *HO* (ChrIV 48,031–46271, encoding homothallic switching endonuclease) (Lv et al., 2016; Voth et al., 2001), *GAL80* (ChrXIII 171,594–172,901, encoding transcriptional regulator involved in the repression of *GAL* genes), and *GAL1-7* (including *GAL1*, ChrII 279,021–280,607; *GAL10*, ChrII 278,352–276,253; and *GAL7*, ChrII 275,527–274,427; encoding galactokinase, UDP-glucose-4-epimerase, and galactose-1-phosphate uridyl transferase, respectively) (Jiang et al., 2017; Ma et al., 2019), by CRISPR/Cas9-mediated genome editing (Figs. S2 and S3), generating SquC1 (Fig. 2A, Table 1). To allow dynamic control of squalene synthesis, the key gene (*tHMG1*) encoding the rate-limiting enzyme was placed under the control of the *GAL* regulation system, which is responsive to glucose concentration in *GAL80* disrupted strains (Xie et al., 2015b). To investigate the squalene production, SquC1 was cultured for 13 d in a 250 mL shaking flask with 50 mL of YPDG, and the fermentation condition was applied to subsequent determination of squalene production unless explicitly stated. As shown in Fig. 2B, SquC1 yielded 1157.42 ± 20.41 mg/L squalene. Furthermore, in view of the key role of HMG-CoA reductase (*tHMG1*) in the MVA pathway, an HMG-CoA reductase from *Silicibacter pomeroyi* (*NADH-HMGR*, highly specific for NADH) (Meadows et al., 2016) was introduced into SquC1, constructing the strain SquC2, which further increased the HMGR activity in the MVA pathway and relaxed the demand for NADPH. The performance of SquC2 for squalene production was further improved to 1358.69 ± 12.96 mg/L and 279.92 ± 7.74 mg/g cdw (cell dry weight) (Fig. 2B and C).

In *S. cerevisiae*, squalene is an intermediate for the biosynthesis of ergosterol, which is an indispensable cell component (Peng et al., 2017). Generally, in native conditions, squalene can be further converted into squalene-2,3-epoxide under the catalysis of squalene epoxidase, encoded by *ERG1* (Fig. 2A). Therefore, to achieve massive production of squalene, the expression of *EGR1* should be downregulated. In this study, repression of *ERG1* was carried out by replacing the native promoter of *ERG1* (P_{ERG1}) with the promoter P_{HXT1} (Fig. 2A, Table 1), which can be repressed when the glucose concentration is low or zero (Ozcan and Johnston, 1995; Zhao et al., 2017). The resulting strain

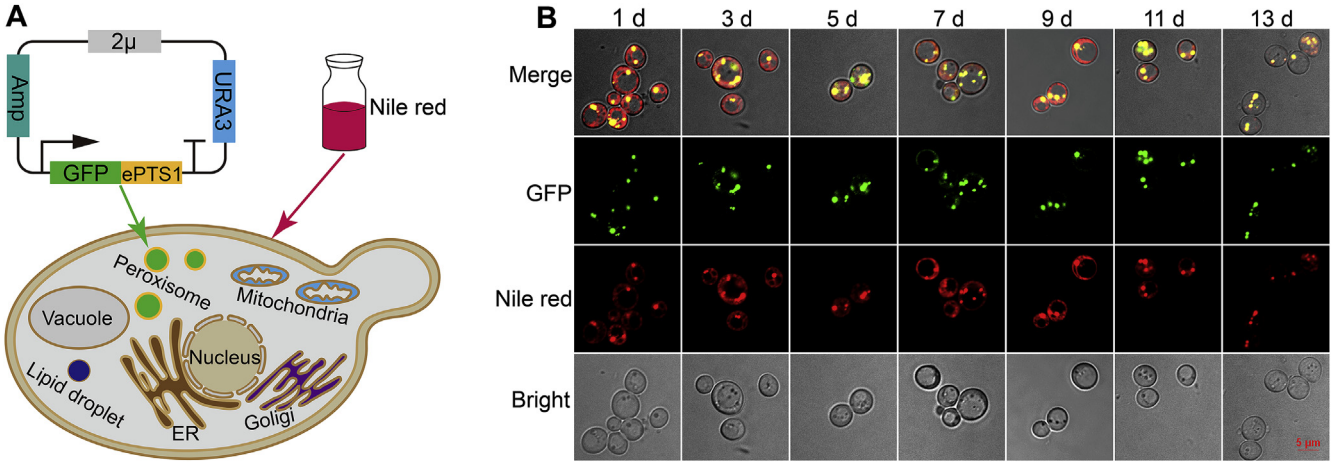

Fig. 1. Investigation of the lipophilic property of peroxisomes. (A) Schematic diagram of experimental design. GFP-ePTS1 is used to specifically mark peroxisomes. Nile red is used to show intracellular lipophilic regions. (B) Lipophilic property observation of peroxisomes in the strain BY4741GE through LSCM. (For interpretation of the references to colour in this figure legend, the reader is referred to the Web version of this article.)

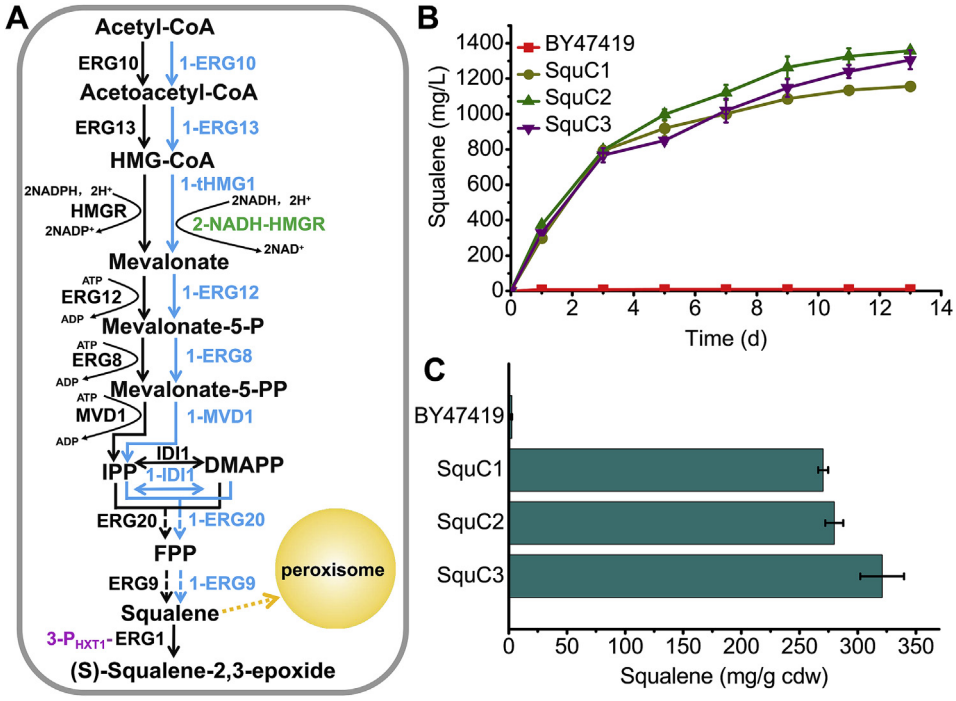

Fig. 2. Squalene overproduction in the cytoplasm of *S. cerevisiae*. (A) Engineering of the squalene synthesis pathway. The native pathway is shown in black. For the engineered pathway, endogenous genes are displayed in blue, and heterologous NADH-HMGR is shown in green. The native promoter of *ERG1* is replaced with the P_{HXT1}, shown in purple. Arabic numerals in front of genes represent the construction order of the engineered strains. Dotted lines represent multiple reactions. The orange dotted line and sphere indicate that squalene could be distributed in peroxisomes. (B) and (C) Squalene accumulation in engineered strains. (For interpretation of the references to colour in this figure legend, the reader is referred to the Web version of this article.)

SquC3 exhibited an improved specific titer of 321.08 ± 18.78 mg/g cdw (Fig. 2C). At this point, we obtained an engineered yeast, which could overproduce squalene in the cytoplasm.

3.2.2. Distribution of squalene overproduced in the cytoplasm

To investigate the distribution of overproduced squalene in the engineered strains, SquC3GE (Table 1) was constructed by introducing GFP-ePTS1 into the corresponding strain and TEM observation was performed first. Analysis of the images of the cytoplasm-engineered strain SquC3GE compared with those of the wild strain BY4741GE revealed the occurrence of large "bubbles" in cells (Fig. 3A). In addition, the "bubbles" tended to fuse and form larger "bubbles" along with increasing squalene production because the supersized "bubbles" might be the most efficient form for product storage in terms of surface-to-volume ratio. These apparent traits showed that these "bubbles" are like a type of LD. Although accumulated squalene was shown to be incorporated into cytoplasmic LDs in some studies (Spanova et al., 2010; Wei et al., 2018), the nature of the "bubbles" was further investigated with LSCM in our work. In contrast to the results of strain BY4741GE (Fig. 1B), giant "bubbles" were clearly observed in SquC3GE in the brightfield images (Fig. 3B), which was consistent with the TEM observations (Fig. 3A). These observations confirmed excessive squalene accumulation in "bubbles". By comparing the fluorescent images of GFP-ePTS1 with the brightfield images, we noticed that the green fluorescent spots mostly overlapped with the "bubbles" in the engineered strain SquC3GE (Fig. 3B). Considering the precise location of GFP-ePTS1 in peroxisomes, we determined that the "bubbles" were inflated peroxisomes, which was attributed to the incorporation of squalene. Based on the above observations, it can be concluded that squalene was reserved in peroxisomes in SquC3GE.

Meanwhile, to further confirm the specific distribution of squalene in peroxisomes, SquC3GE was stained with Nile red. Comparison of the fluorescent images of GFP-ePTS1 with the Nile red staining results showed that after fermentation for 1 d, the green fluorescent spots overlapped with the red spots (Fig. 3B). However, as the fermentation process proceeded (3 d–13 d), some "black holes" emerged in the Nile red images, which surprisingly overlapped with the "bubbles". To further understand these "black holes", the maximum excitation and emission wavelengths and fluorescence intensity of Nile red dissolved in different concentrations of squalene were detected with a microplate reader. It was shown that the maximum excitation and emission wavelengths did not shift with changes in squalene concentration (Fig. 3C and D). However, low concentrations of squalene (5% and 10%) increased the fluorescence intensity of Nile red, whereas high concentrations of squalene (40%, 80% and 99%) greatly decreased the fluorescence intensity (Fig. 3E). This observation indicated that the "black holes" should be the regions containing high concentrations of squalene, which attenuated the red fluorescence of Nile red. Because the positions of the "black holes" in the Nile red images were consistent with those of the green fluorescent spots (peroxisomes) and the "bubbles", it can be concluded that the overproduced squalene in *S. cerevisiae* was stored in peroxisomes. Although extensive squalene was reserved in peroxisomes, cell growth of the engineered strains was rarely affected (Fig. S4A). All of these results indicated that the yeast peroxisome is an advantageous dynamic depot for storing hydrophobic compounds.

3.3. Yeast peroxisome as an efficient subcellular factory for squalene biosynthesis

3.3.1. Compartmentalization of squalene synthesis in peroxisomes

To explore the potential of the peroxisome as a compartment for the synthesis of terpenes, the entire engineered squalene synthesis pathway, including ten genes (*ERG10*, *ERG13*, *tHMG1*, *NADH-HMGR*, *ERG12*, *ERG8*, *MVD1*, *IDI1*, *ERG20*, *ERG9*) fused with C-terminal ePTS1, was overexpressed in BY47419 (Fig. 4A), generating recombinant strain SquP1 (Table 1). Without significantly altered growth (Fig. S4B), this strain produced squalene at 655.84 ± 24.64 mg/L (Fig. 4B), representing a 68-fold increase relative to BY47419.

To further improve squalene production, native P_{ERG1} was also replaced with P_{HXT1} in SquP1 to construct SquP2 (Fig. 4A, Table 1). As shown in Fig. 4B, SquP1 and SquP2 produced similar amounts of squalene (655.84 ± 24.64 mg/L versus 680.14 ± 39.33 mg/L), and the specific titer of squalene changed only from 139.67 ± 6.02 mg/g cdw to 176.5 ± 9.74 mg/g cdw (Fig. 4C). This might be due to the fact that most of squalene was stored in peroxisomes and the cytosolic accumulation of squalene should be very limiting. Therefore, *ERG1* downregulation was not working well for improving overall squalene

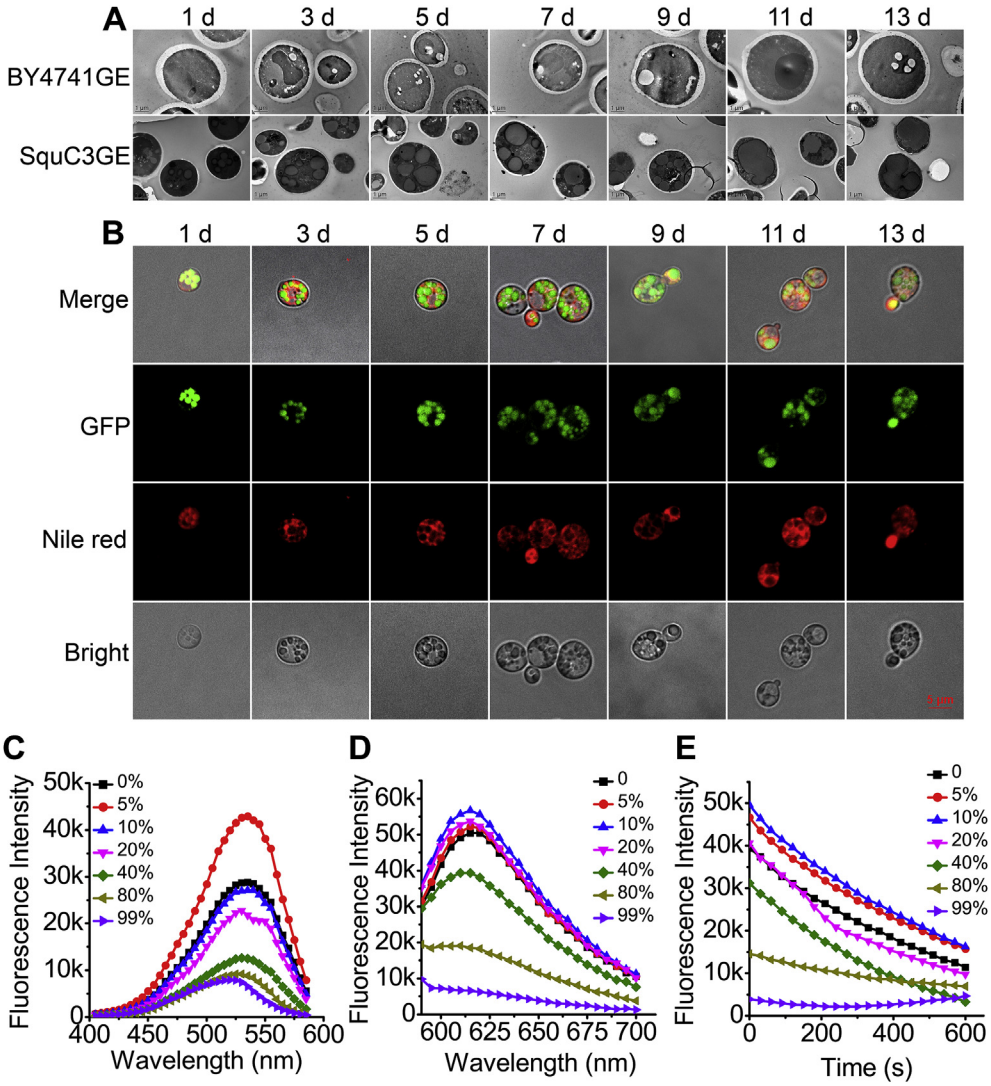

Fig. 3. Squalene distribution in the engineered strain SquC3GE. (A) Distribution analysis of squalene by TEM. (B) Distribution analysis of squalene by LSCM (C) Excitation wavelength scanning of Nile red in different concentrations of squalene at an emission wavelength of 615 nm. (D) Emission wavelength scanning of Nile red in different concentrations of squalene at an excitation wavelength of 561 nm. (E) Fluorescence intensity detection of Nile red in different concentrations of squalene at excitation and emission wavelengths of 561 nm and 615 nm, respectively. (For interpretation of the references to colour in this figure legend, the reader is referred to the Web version of this article.)

titer, but instead, inhibited cell growth (Fig. S4B) due to the affected ergosterol synthesis. In addition, it has been shown that *GPD*1 and *GPD2* encode the rate-limiting enzymes (glycerol-3-phosphate dehydrogenases) for glycerol formation (Lian et al., 2014), which could result in loss of carbon sources. Hence, to eliminate consumption of carbon sources, *GPD1* and *GPD2* were disrupted in SquP2, generating SquP3 (Table 1). However, the squalene titer of SquC3 was not improved (674.98 ± 32.69 mg/L) (Fig. 4B). In view of the important roles of *tHMG1* and *IDI1* in the MVA pathway (Ignea et al., 2014; Polakowski et al., 1998), both genes were simultaneously overexpressed with C-terminal ePTS1 and integrated into *GPD1* and *GPD2* sites in one or two copies, generating SquP4 and SquP5, respectively (Table 1). The accumulation of squalene in SquP4 and SquP5 gradually increased from 706.26 ± 34.94 mg/L to 794.91 ± 31.12 mg/L (Fig. 4B). However, further increasing the copy numbers of the two genes was no longer a feasible method to improve the squalene output (data not shown).

3.3.2. Engineering ATP and NADPH supply for peroxisomes

Synthesis of squalene from acetyl-CoA led to extensive consumption of ATP and NADPH (Fig. 4A). Ant1p, a peroxisomal adenine nucleotide transporter, is an integral protein of the peroxisomal membrane and is responsible for transferring ATP into peroxisomes for β-oxidation of medium-chain fatty acids (van Roermund et al., 2001). The isocitrate-2-oxoglutarate redox shuttle consists of peroxisomal (Idp3p) and cytosolic (Idp2p) isocitrate dehydrogenases, interconnecting the cytosolic and peroxisomal pools of NADPH (Roermund et al., 2014). To enhance the supply of ATP to peroxisomal squalene synthesis, *ANT1* was overexpressed in SquP5, generating SquP6 (Fig. 4A, Table 1), and the squalene titer increased to 1009.78 ± 43.76 mg/L (242.08 ± 10.33 mg/g cdw) (Fig. 4B and C). Furthermore, to provide adequate NADPH to the squalene synthesis pathway compartmentalized in peroxisomes, *IDP2* and *IDP3* were overexpressed in SquP6, generating SquP7 (Fig. 4A, Table 1). Squalene production of SquP7 was further improved to 1174.94 ± 22.01 mg/L (269.32 ± 1.91 mg/g cdw) (Fig. 4B and C). These results demonstrated that the peroxisome internal ATP and NADPH levels were not enough for the squalene biosynthesis pathway compartmentalized in peroxisomes and that increasing the transport of ATP and NADPH into peroxisomes is an effective strategy to improve the supply of ATP and NADPH for squalene synthesis in peroxisomes.

3.3.3. Engineering acetyl-CoA supply for peroxisomes

Acetyl-CoA served as the precursor for squalene biosynthesis (Fig. 4A). It has been suggested that an increased acetyl-CoA pool can improve the biosynthesis of downstream terpenes (Paramasivan and Mutturi, 2017). In *S. cerevisiae*, the glyoxylate shunt could transfer acetyl-CoA from peroxisomes into mitochondria, resulting in loss of peroxisomal acetyl-CoA. In the glyoxylate shunt process, Cit2p, located in peroxisomes, catalyzes the condensation of acetyl-CoA with

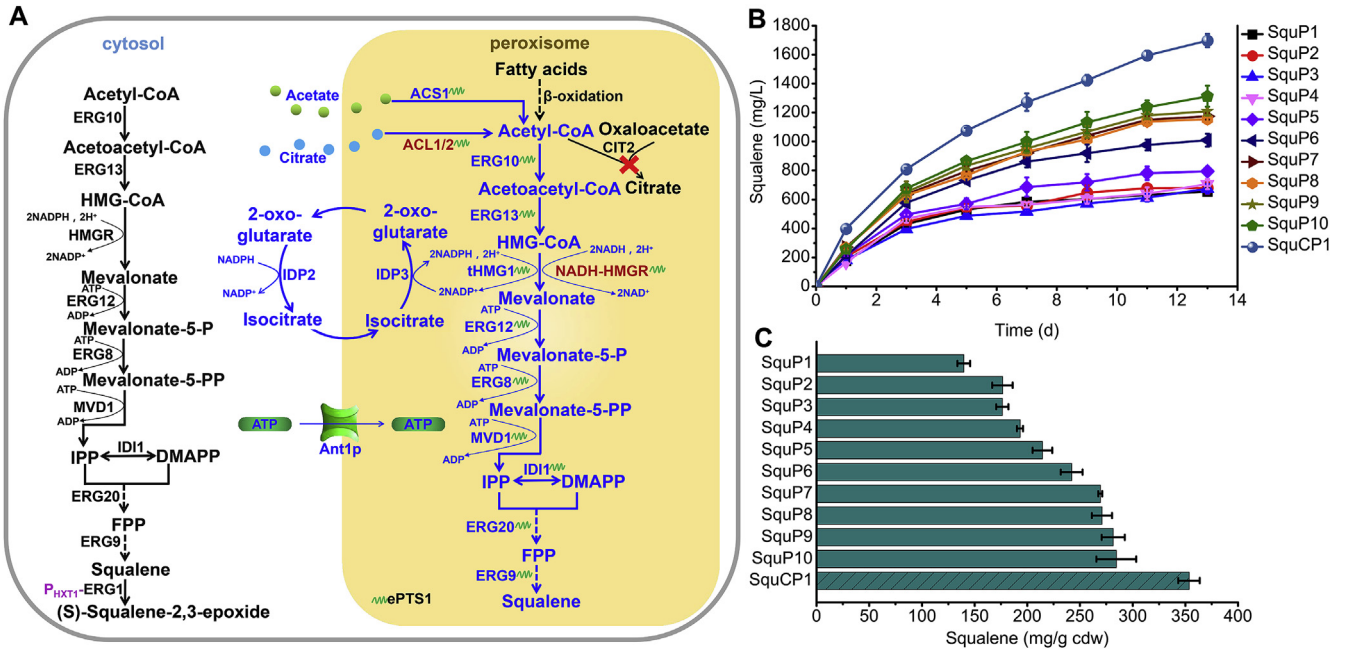

Fig. 4. Squalene biosynthesis compartmentalized in the peroxisomes of *S. cerevisiae*. (A) Engineering of the compartmentalized pathway. The native pathway in the cytoplasm is shown in black. For the engineered pathway, each gene was fused with a C-terminal ePTS1 tag. Endogenous genes are displayed in dark blue, and heterologous genes in dark red. The native promoter of *ERG1* is replaced with the P_{HXT1}, shown in purple. Green and light blue spheres represent acetate and citrate, respectively. (B) and (C) Squalene accumulation in engineered strains. (For interpretation of the references to colour in this figure legend, the reader is referred to the Web version of this article.)

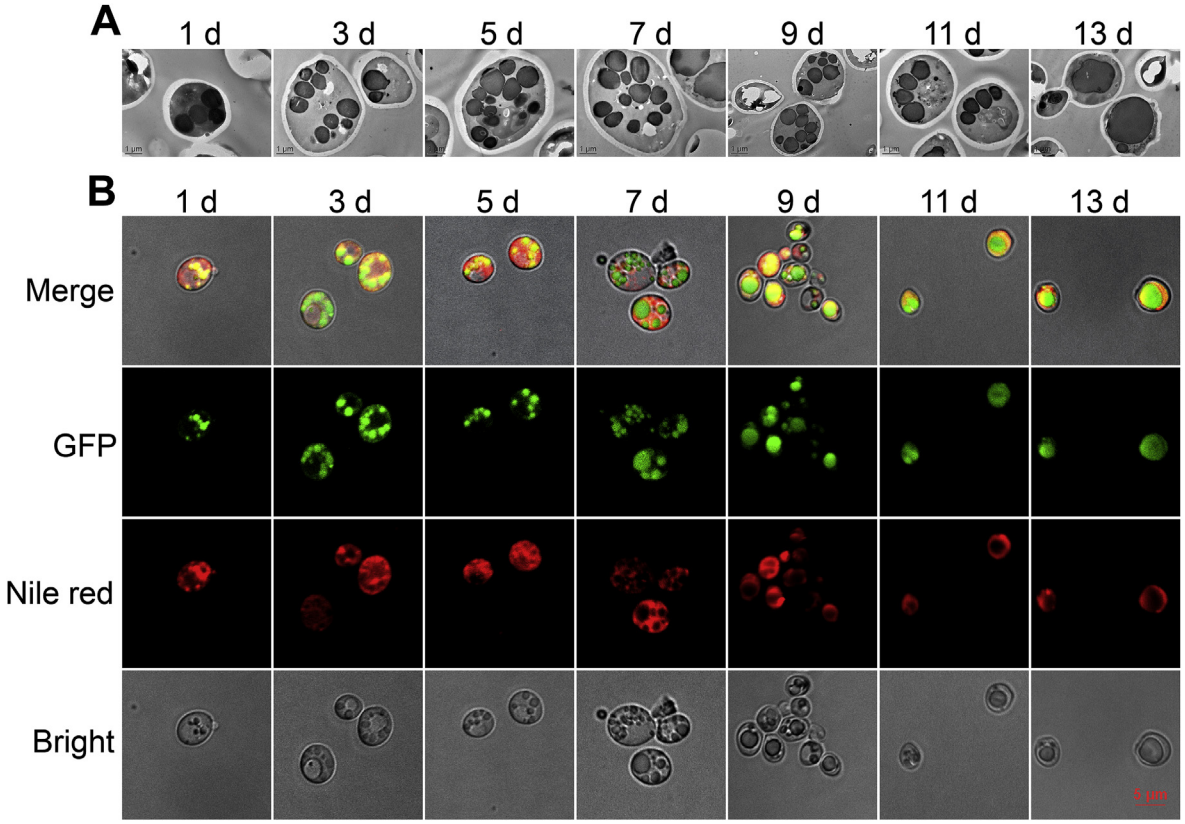

Fig. 5. Squalene distribution in the engineered strain SquP10 GE. (A) Analysis of squalene distribution by TEM. (B) Analysis of squalene distribution by LSCM.

oxaloacetate (Chen et al., 2012). To reduce the loss of peroxisomal acetyl-CoA, *CIT2* was deleted to construct SquP8 (Fig. 4A, Table 1). The squalene titer of SquP8 was 1154.69 ± 25.61 mg/L, which was not improved relative to the host strain SquP7 (Fig. 4B), indicating that the loss of acetyl-CoA might not be a critical issue. Although the engineering of acetyl-CoA synthesis in the cytoplasm has been well studied (Chen et al., 2013; Lian et al., 2014), the impermeability of the peroxisomal membrane to acetyl-CoA (DeLoache et al., 2016;

Roermund et al., 1995) makes it impossible to improve the acetyl-CoA supply to the peroxisome by enhancing the synthesis of this molecule in the cytosol. Additionally, although β-oxidation of fatty acids could supply a certain amount of acetyl-CoA to peroxisomes, acetyl-CoA from this resource might be limited for squalene output because the β-oxidation of fatty acids in *S. cerevisiae* is usually not prosperous. In addition, cytoplasmic acetate can pass into peroxisomes and further be ligated with CoA into acetyl-CoA, which is catalyzed by acetyl-CoA synthetase (Acs1p) (Chen et al., 2012). Hence, to provide more acetyl-CoA to peroxisomes, *ACS1-ePTS1* was overexpressed in SquP8 to construct SquP9 (Fig. 4A, Table 1). As illustrated in Fig. 4B and C, the specific squalene titer of SquP9 increased from 270.88 ± 9.65 mg/g cdw (SquP8) to 281.59 ± 11.00 mg/g cdw, demonstrating that acetate may be a considerable precursor for engineering supply of peroxisomal acetyl-CoA. In addition, ATP-dependent citrate lyase (*ACL*) catalyzes the generation of cytosolic acetyl-CoA from citrate (Lian et al., 2014), which can penetrate the peroxisomal membrane (Chen et al., 2012; DeLoache et al., 2016). To further increase the acetyl-CoA supply to the peroxisome, *YlALC1*-ePTS1 and *YlACL2*-ePTS1 (ACL genes from *Yarrowia lipolytica*) (Lian et al., 2014) were cloned and introduced into SquP9 (Fig. 4A, Table 1). The resulting strain, SquP10, produced 1312.82 ± 73.09 mg/L (284.45 ± 18.93 mg/g cdw) squalene (Fig. 4B and C), suggesting that the productivity of SquP10 was finitely improved. Hereto, we achieved high production of squalene in yeast peroxisomes.

3.3.4. Distribution of squalene overproduced in peroxisomes

To investigate the distribution of squalene overproduced in yeast peroxisomes, SquP10 GE was constructed and subsequently observed through TEM. As shown in Fig. 5A, similar to the TEM results of SquC3GE, “large bubbles” also appeared in the cytosol of SquP10 GE, implying that the overproduced squalene might be reserved in peroxisomes. To further determine the distribution of squalene, SquP10 GE was stained with Nile red and observed with LSCM. As illustrated in Fig. 5B, “large bubbles” could be observed as well in the brightfield images. Furthermore, “black holes” in the Nile red images exactly overlapped with green fluorescent spots and “bubbles”, which is consistent with the results of SquC3GE, suggesting that the squalene overproduced in peroxisomes was simultaneously reserved in peroxisomes. These results revealed that yeast peroxisome can be utilized as not only a dynamic storage depot for hydrophobic chemicals but also a variable and superior subcellular factory for terpene biosynthesis.

3.4. Dual cytoplasmic-peroxisomal engineering to overproduce squalene

Encouraged by the superiority of yeast peroxisomes as storage depots and subcellular factories, we intended to harness peroxisomes to build an engineered yeast strain with high squalene output. As previously reported (Lv et al., 2016), taking full advantage of the productivity of multiple compartments led to a dramatic enhancement in product titer. In addition, hybrid strains have been extensively recognized as bearing higher stresses than haploid strains (Yao et al., 2018). Therefore, to further improve squalene production, hybridization of the cytoplasm- and peroxisome-engineered strains was explored (Fig. 6A). In order to hybridize with SquP10, the mating type of SquC3 was first switched from a-type to α-type, resulting in SquC4 (Table 1). Then, SquCP1 (Table 1) was created by hybridizing SquC4 with SquP10. As shown in Fig. 4B, an obvious improvement in squalene titer (1698.02 ± 45.88 mg/L) was obtained in the hybrid strain, representing an increase of approximately 29.34% and 29.97% relative to the parent strains SquP10 and SquC3, respectively. Moreover, the cell growth was almost identical to that of SquP10 and improved by 17.98% compared with that of SquC3 (Fig. S4B). In addition, the specific squalene titer of the hybrid strain was enhanced to 353.47 ± 10.12 mg/g cdw, representing a 10.09% and 24.26% increase compared to the specific titer of the parent strains SquC3 and SquP10, respectively (Fig. 4C). These results suggested that dual cytoplasmic-peroxisomal engineering is an effective strategy to improve squalene biosynthesis in *S. cerevisiae*.

To further evaluate the performance of the diploid strain in our study, fed-batch fermentation was performed in a 5 L bioreactor. Because the auxotrophic strains were not suitable for high-cell-density fermentation (Xie et al., 2015a), the *URA3*, *MET15*, *LEU2* and *HIS3* markers were complemented into SquC4 and SquP10, generating SquC5 and SquP11, respectively (Table 1). SquCP2 (Table 1), a hybrid strain complemented with auxotroph markers, was built by mating SquC5 with SquP11 and used for subsequent fed-batch fermentation. Cell growth and inducible expression of the rate-limiting enzyme of the engineered pathways were separated through a two-stage fermentation strategy. In the first fermentation stage, glucose was fed as the initial carbon source to maintain rapid cell growth and inhibit the expression of the rate-limiting enzyme, HMG-CoA reductase, of the engineered pathways. In the second stage, ethanol was added to meet the demand of the carbon source, and the engineered pathway began to work efficiently because the repression of the *GAL* promoters was alleviated after glucose depletion. The results showed that two-stage fed-batch fermentation further elevated squalene production, yielding an overall 11.00 g/L squalene at a cell density (OD600) of 124.74 at 168 h (Fig. 6B).

4. Discussion

The subcellular distribution of terpenes in the cell greatly influences the terpene accumulation and tolerance of organisms. In this study, we reported that the yeast peroxisome is equipped with the ability to reserve extensive squalene, which makes the peroxisome an outstanding intracellular storage depot for hydrophobic chemicals. Furthermore, we showed that the squalene synthesis pathway compartmentalized in peroxisomes could work efficiently and resulted in massive squalene production, demonstrating that the yeast peroxisome is also an excellent subcellular factory for synthetic biology. Finally, we obtained a hybridized yeast through combining cytoplasm engineering and peroxisome compartmentalization, increasing squalene output to 11.00 g/L in fed-batch fermentation, which is the highest ever reported.

Previous studies have suggested that large hydrophobic molecules that accumulate intracellularly, such as TAG, squalene and lycopene, are probably reserved in LDs (Ferreira et al., 2018; Ma et al., 2019; Wei et al., 2018). However, LDs might be not ideal storage compartments in *S. cerevisiae*, because the biosynthesis of storage lipids in this non-oleaginous host (Zhou et al., 2014) is limited. Interestingly, in this study, through TEM and LSCM, we observed strong evidence supporting a new dynamic depot for squalene storage, the peroxisome, in both a cytoplasm-engineered strain and a peroxisome-compartmentalized strain. For the peroxisome-engineered strain, it is not difficult to understand the storage of squalene in the peroxisomes because squalene synthesis was compartmentalized in the peroxisomes. However, why and how cytoplasm-synthesized squalene was able to reach and be assembled in peroxisomes remain unknown. A possible explanation is that squalene synthesis occurs around the endoplasmic reticulum (ER), where squalene synthetase is located (Peng et al., 2017), and peroxisomes are formed from the ER as well (Yuan et al., 2016), thus enabling convenient localization of squalene in peroxisomes. In addition, in this study, the peroxisomal matrix was shown to be lipophilic, endowing peroxisomes with the capability to store squalene. Other mechanisms for lipid transport and storage, such as protein-mediated transport or membrane contact, may also be anticipated. Our results can be regarded as demonstrating a novel aspect of squalene storage and featuring the yeast peroxisome as a predominant dynamic storage depot for lipophilic chemicals. This work may inspire researchers to examine the positioning of other lipids, and lays the groundwork for understanding the mechanisms of the distribution, transport and storage of other intracellular hydrophobic compounds. Furthermore, we observed

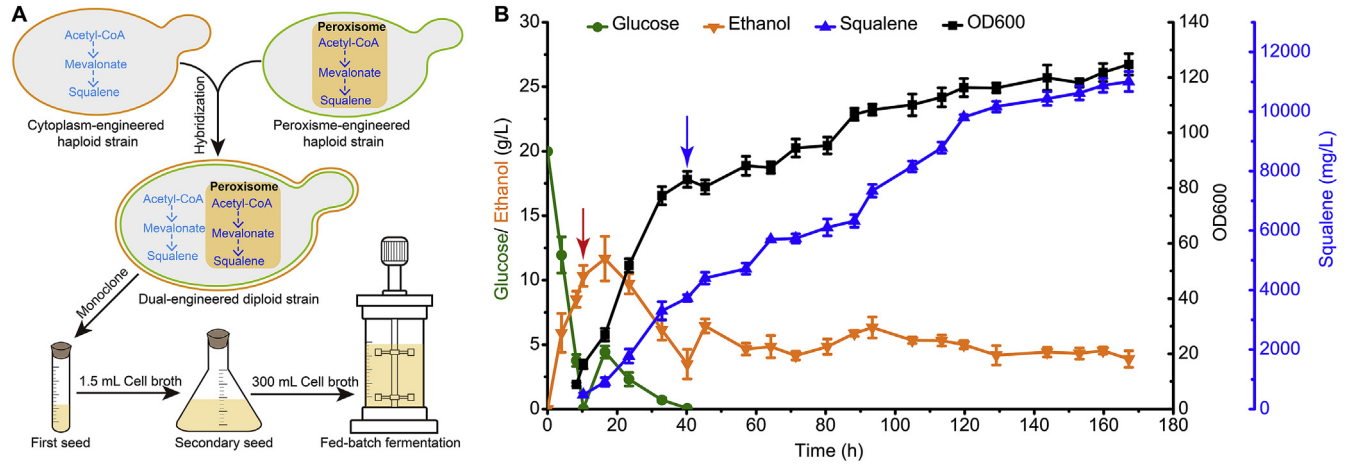

Fig. 6. Dual cytoplasmic-peroxisomal engineering for squalene overproduction. (A) Schematic diagram of dual cytoplasmic-peroxisomal engineering and the process of fed-batch fermentation. (B) High-density fermentation for squalene production. Time courses showing changes in cell growth and squalene production of SquCP2 during fed-batch fermentation. The red arrow represents the feed of glucose into the medium. The blue arrow represents the feed of ethanol into the medium. (For interpretation of the references to colour in this figure legend, the reader is referred to the Web version of this article.)

that the size and number of peroxisomes changed with the accumulation of intracellular squalene, endowing the engineered strains with high storage capacity, which might be another important reason why a high squalene titer was achieved in our engineered strains. In addition, during the investigation of the subcellular distribution of squalene, an unexpected experimental phenomenon was observed, that is, the red fluorescence of Nile red was attenuated by high concentrations of squalene, which might be due to the effects of the changes in polarity and viscosity at high concentrations of squalene on Nile red (Dutt and Sachdeva, 2003; Yablon and Schilowitz, 2004). We suggest that this attenuating phenomenon should also be considered when other neutral lipids are stained with Nile red.

Pathway compartmentalization has been recently developed as a promising approach to enhance product titer. To date, most of the best examples of subcellular metabolic engineering of terpene synthesis have focused on mitochondria (Lv et al., 2016; Yee et al., 2019; Yuan and Ching, 2016) and ER (Arendt et al., 2017; Kim et al., 2019). Compartmentalization of terpene synthesis in mitochondria could ensure sufficient acetyl-CoA supply, limit metabolic crosstalk and improve pathway efficiency. Expansion of ER by overexpressing key ER size regulatory factor *INO2* or disrupting phosphatidic acid phosphatase-encoding *PAH1* could stimulate the production of ER-localized proteins, resulting in the increased accumulation of related metabolites (Arendt et al., 2017; Kim et al., 2019). However, as the indispensable cellular engine, mitochondria may be not suitable as a compartment for storing massive hydrophobic compounds. As to ER, accumulation of extensive hydrophobic chemicals in the lumen of ER may affect its function in synthesizing and folding proteins. Here, inspired by the advantages of *S. cerevisiae* peroxisomes as dynamic storage depots, we systematically explored the possibility of using peroxisomes as another candidate to compartmentalize squalene synthesis. The peroxisome-compartmentalized strain SquP1 produced 655.84 mg/L squalene, exhibiting more than a 68-fold improvement relative to the host strain, demonstrating the potential capacity of peroxisome engineering in terpenoid synthesis. In previous research on subcellular compartmentalization, a substantial decrease in the cell growth of the recombinant strains was always observed, mainly due to the heavy burden of multigene overexpression for organelles and the cytotoxicity associated with intermediate accumulation (Lv et al., 2016). However, the biomass of peroxisome-engineered strains was well maintained, enabling high production of squalene. We deduced that this effect could be chiefly attributed to the ability of peroxisomes to ease the burden of the heterogeneous pathway by regulating their size and number in response to product synthesis. In addition, we deliberately strengthened the downstream portion of the MVA pathway so that intermediates could be converted to the low-toxicity compound squalene (Spanova et al., 2010) in a timely manner.

However, the peroxisome-engineered strain SquP1 produced less squalene than the cytoplasm-engineered strain SquC2. The biosynthesis of squalene requires sufficient ATP and NADPH, and the transport of these molecules to peroxisomes has been shown to be induced by fatty acids (Roermund et al., 2014; van Roermund et al., 2001), which are noncommon feedstocks for industrial production and were not added to our fermentation medium. Hence, we hypothesize that the low squalene titer in SquP1 might be attributed to insufficient peroxisomal ATP and NADPH levels. To alleviate the effects of the possible limitation of these factors in peroxisome-engineered strains, a promising strategy was applied to enhance the transport of ATP and NADPH to the engineered pathway in peroxisomes, and as expected, considerable improvement in squalene production was achieved, demonstrating that providing sufficient ATP and NADPH is an efficacious strategy to improve peroxisome-compartmentalized squalene biosynthesis. Furthermore, it has been proposed in many studies that enhanced acetyl-CoA levels could improve the downstream biosynthesis of terpenes (Li et al., 2019; Paramasivan and Mutturi, 2017). In view of the possible finite acetyl-CoA resources in peroxisomes, *ACS1-ePTS1*, *YlACL1-ePTS1* and *YlACL2-ePTS1* were overexpressed to increase the acetyl-CoA supply in peroxisomes, but the squalene titer improved only slightly (Fig. 4B and C). We speculated that the weak improvement in squalene synthesis was due to the insufficient acetate and citrate supply to peroxisomes (Rodriguez et al., 2016; Shiba et al., 2007). Because peroxisomes share a common pool of small metabolites with the cytoplasm (Antonenkov and Hiltunen, 2012), increased abundance of acetate and citrate in peroxisomes might be achieved by enhancing the accumulation of these molecules in the cytoplasm in the future work.

Considering the advantages of the peroxisome as a storage depot and a subcellular factory and the excellent cell growth of diploid strains over haploid strains (Lv et al., 2016), dual cytoplasmic-peroxisomal engineering was performed by combining cytoplasm- and peroxisome-engineered strains to obtain a high-producing squalene strain. Squalene production in SquCP1 (1698.02 mg/L) was clearly increased relative to that in SquC3 (1306.49 mg/L) and SquP10 (1312.82 mg/L). Moreover, the biomass of SquCP1 (OD600 11.94) was improved over that of SquC3 (OD600 10.12) and SquP10 (OD600 11.47), probably because diploid strains usually exhibit high stress tolerance (Li et al., 2010) or because the resources for the proliferation of diploid cells might be better guaranteed as a result of the significant reduction in cell wall components in diploid strains (de Godoy et al., 2008). The high specific squalene titer of SquCP1 suggested that the increased squalene

production in the diploid strain was not due solely to improved cell growth but was also associated with the complete utilization of the production capacity of the cytoplasm and peroxisomes. In addition, diploid strains generally have larger cell volumes, which might endow diploid cells with increased storage space for intracellular squalene (de Godoy et al., 2008).

In conclusion, this study indicated that peroxisomes of *S. cerevisiae* hold great promise in synthetic biology: (i) with rapid and effective protein import machinery, enzymes of metabolic pathways can be directly compartmentalized into peroxisomes; (ii) peroxisomes can store high levels of squalene, as the size and number of peroxisomes can be adjusted according to growth state, providing the novel possibility of the storage of other valuable hydrophobic chemicals; and (iii) mating of cytoplasm- and peroxisome-engineered haploids offers high productivity of compounds of interest in yeast.

Declaration of competing interest

The authors declare no competing interests.

Acknowledgements

This work was financially supported by the National Natural Science Foundation of China (No. 31772007 and No. 21776075) and the Fundamental Research Funds for the Central University of China (No. 22221818014).

Appendix A. Supplementary data

Supplementary data to this article can be found online at https://doi.org/10.1016/j.ymben.2019.11.001.

References

Antonenkov, V.D., Hiltunen, J.K., 2012. Transfer of metabolites across the peroxisomal membrane. Bba-Mol Basis Dis. 1822, 1374–1386.
Arendt, P., Miettinen, K., Pollier, J., De Rycke, R., Callewaert, N., Goossens, A., 2017. An endoplasmic reticulum-engineered yeast platform for overproduction of triterpenoids. Metab. Eng. 40, 165–175.
Banerjee, A., Sharkey, T.D., 2014. Methylerythritol 4-phosphate (MEP) pathway metabolic regulation. Nat. Prod. Rep. 31, 1043–1055.
Bian, G.K., Deng, Z.X., Liu, T.G., 2017. Strategies for terpenoid overproduction and new terpenoid discovery. Curr. Opin. Biotechnol. 48, 234–241.
Brennan, T.C.R., Turner, C.D., Kromer, J.O., Nielsen, L.K., 2012. Alleviating monoterpene toxicity using a two-phase extractive fermentation for the bioproduction of jet fuel mixtures in *Saccharomyces cerevisiae*. Biotechnol. Bioeng. 109, 2513–2522.
Chen, Y., Daviet, L., Schalk, M., Siewers, V., Nielsen, J., 2013. Establishing a platform cell factory through engineering of yeast acetyl-CoA metabolism. Metab. Eng. 15, 48–54.
Chen, Y., Siewers, V., Nielsen, J., 2012. Profiling of cytosolic and peroxisomal acetyl-CoA metabolism in *Saccharomyces cerevisiae*. PLoS One 7.
Choi, S.Y., Sim, S.J., Choi, J.I., Woo, H.M., 2018. Identification of small droplets of photosynthetic squalene in engineered *Synechococcus elongatus* PCC 7942 using TEM and selective fluorescent Nile red analysis. Lett. Appl. Microbiol. 66, 523–529.
de Godoy, L.M.F., Olsen, J.V., Cox, J., Nielsen, M.L., Hubner, N.C., Frohlich, F., Walther, T.C., Mann, M., 2008. Comprehensive mass-spectrometry-based proteome quantification of haploid versus diploid yeast. Nature 455 1251-U60.
DeLoache, W.C., Russ, Z.N., Dueber, J.E., 2016. Towards repurposing the yeast peroxisome for compartmentalizing heterologous metabolic pathways. Nat. Commun. 7, 11.
Dutt, G.B., Sachdeva, A., 2003. Temperature-dependent rotational relaxation in a viscous alkane: interplay of shape factor and boundary condition on molecular rotation. J. Chem. Phys. 118, 8307–8314.
Ferreira, R., Teixeira, P.G., Gossing, M., David, F., Siewers, V., Nielsen, J., 2018. Metabolic engineering of *Saccharomyces cerevisiae* for overproduction of triacylglycerols. Metab. Eng. Commun. 6, 22–27.
Ignea, C., Pontini, M., Maffei, M.E., Makris, A.M., Kampranis, S.C., 2014. Engineering monoterpene production in yeast using a synthetic dominant negative geranyl diphosphate synthase. ACS Synth. Biol. 3, 298–306.
Jiang, G.Z., Yao, M.D., Wang, Y., Zhou, L., Song, T.Q., Liu, H., Xiao, W.H., Yuan, Y.J., 2017. Manipulation of GES and ERG20 for geraniol overproduction in *Saccharomyces cerevisiae*. Metab. Eng. 41, 57–66.
Joshi, A.S., Cohen, S., 2019. Lipid droplet and peroxisome biogenesis: do they go hand-in-hand? Front Cell Dev. Biol. 7.
Kim, J.-E., Jang, I.-S., Son, S.-H., Ko, Y.-J., Cho, B.-K., Kim, S.C., Lee, J.Y., 2019. Tailoring the *Saccharomyces cerevisiae* endoplasmic reticulum for functional assembly of terpene synthesis pathway. Metab. Eng. 56, 50–59.
Klei, I.J., Van der Veenhuis, M., 1997. Yeast peroxisomes: function and biogenesis of a versatile cell organelle. Trends Microbiol. 5, 502–509.
Kohlwein, S.D., Veenhuis, M., van der Klei, I.J., 2013. Lipid droplets and peroxisomes: key players in cellular lipid homeostasis or A matter of fat-store 'em up or burn 'em down. Genetics 193, 1–50.
Lane, S., Zhang, S.Y., Wei, N., Rao, C., Jin, Y.S., 2015. Development and physiological characterization of cellobiose-consuming *Yarrowia lipolytica*. Biotechnol. Bioeng. 112, 1012–1022.
Larroude, M., Celinska, E., Back, A., Thomas, S., Nicaud, J.-M., Ledesma-Amaro, R., 2018. A synthetic biology approach to transform *Yarrowia lipolytica* into a competitive biotechnological producer of beta-carotene. Biotechnol. Bioeng. 115, 464–472.
Li, B.Z., Cheng, J.S., Ding, M.Z., Yuan, Y.J., 2010. Transcriptome analysis of differential responses of diploid and haploid yeast to ethanol stress. J. Biotechnol. 148, 194–203.
Li, M., Hou, F., Wu, T., Jiang, X., Li, F., Liu, H., Xian, M., Zhang, H., 2019. Recent advances of metabolic engineering strategies in natural isoprenoid production using cell factories. Nat. Prod. Rep. https://doi.org/10.1039/C9NP00016J.
Li, Y.H., Zhao, Z.B., Bai, F.W., 2007. High-density cultivation of oleaginous yeast *Rhodosporidium toruloides* Y4 in fed-batch culture. Enzym. Microb. Technol. 41, 312–317.
Lian, J.Z., Si, T., Nair, N.U., Zhao, H.M., 2014. Design and construction of acetyl-CoA overproducing *Saccharomyces cerevisiae* strains. Metab. Eng. 24, 139–149.
Lv, X.M., Wang, F., Zhou, P.P., Ye, L.D., Xie, W.P., Xu, H.M., Yu, H.W., 2016. Dual regulation of cytoplasmic and mitochondrial acetyl-CoA utilization for improved isoprene production in *Saccharomyces cerevisiae*. Nat. Commun. 7, 12.
Ma, T., Shi, B., Ye, Z.L., Li, X.W., Liu, M., Chen, Y., Xia, J., Nielsen, J., Deng, Z.X., Liu, T.G., 2019. Lipid engineering combined with systematic metabolic engineering of *Saccharomyces cerevisiae* for high-yield production of lycopene. Metab. Eng. 52, 134–142.
Martinez, J.L., Sanchez, M.B., Martinez-Solano, L., Hernandez, A., Garmendia, L., Fajardo, A., Alvarez-Ortega, C., 2009. Functional role of bacterial multidrug efflux pumps in microbial natural ecosystems. FEMS Microbiol. Rev. 33, 430–449.
Meadows, A.L., Hawkins, K.M., Tsegaye, Y., Antipov, E., Kim, Y., Raetz, L., Dahl, R.H., Tai, A., Mahatdejkul-Meadows, T., Xu, L., Zhao, L.S., Dasika, M.S., Murarka, A., Lenihan, J., Eng, D., Leng, J.S., Liu, C.L., Wenger, J.W., Jiang, H.X., Chao, L.L., Westfall, P., Lai, J., Ganesan, S., Jackson, P., Mans, R., Platt, D., Reeves, C.D., Saija, P.R., Wichmann, G., Holmes, V.F., Benjamin, K., Hill, P.W., Gardner, T.S., Tsong, A.E., 2016. Rewriting yeast central carbon metabolism for industrial isoprenoid production. Nature 537 694-+.
Moser, S., Pichler, H., 2019. Identifying and engineering the ideal microbial terpenoid production host. Appl. Microbiol. Biotechnol. 103, 5501–5516.
Naziri, E., Mantzouridou, F., Tsimidou, M.Z., 2011. Enhanced squalene production by wild-type *Saccharomyces cerevisiae* strains using safe chemical means. J. Agric. Food Chem. 59, 9980–9989.
Ozcan, S., Johnston, M., 1995. Three different regulatory mechanisms enable yeast hexose transporter (HXT) genes to be induced by different levels of glucose. Mol. Cell. Biol. 15, 1564–1572.
Paramasivan, K., Mutturi, S., 2017. Progress in terpene synthesis strategies through engineering of *Saccharomyces cerevisiae*. Crit. Rev. Biotechnol. 37, 974–989.
Peng, B.Y., Plan, M.R., Chrysanthopoulos, P., Hodson, M.P., Nielsen, L.K., Vickers, C.E., 2017. A squalene synthase protein degradation method for improved sesquiterpene production in *Saccharomyces cerevisiae*. Metab. Eng. 39, 209–219.
Polakowski, T., Stahl, U., Lang, C., 1998. Overexpression of a cytosolic hydroxymethylglutaryl-CoA reductase leads to squalene accumulation in yeast. Appl. Microbiol. Biotechnol. 49, 66–71.
Rodriguez, S., Denby, C.M., Van Vu, T., Baidoo, E.E.K., Wang, G., Keasling, J.D., 2016. ATP citrate lyase mediated cytosolic acetyl-CoA biosynthesis increases mevalonate production in *Saccharomyces cerevisiae*. Microb. Cell Factories 15.
Van Roermund, C.W., Elgersma, Y., Singh, N., Wanders, R.J., Tabak, H.F., 1995. The membrane of peroxisomes in *Saccharomyces cerevisiae* is impermeable to NAD(H) and acetyl-CoA under in vivo conditions. EMBO J. 14, 3480–3486.
Van Roermund, C.W., Hettema, E.H., Kal, A.J., Berg, M., Van den Tabak, H.F., Wanders, R.J., 2014. Peroxisomal beta-oxidation of polyunsaturated fatty acids in Saccharomyces cerevisiae: isocitrate dehydrogenase provides NADPH for reduction of double bonds at even positions. EMBO J. 17, 677–687.
Rucktaschel, R., Girzalsky, W., Erdmann, R., 2011. Protein import machineries of peroxisomes. Bba-Biomembranes 1808, 892–900.
Saraya, R., Veenhuis, M., van der Klei, I.J., 2010. Peroxisomes as dynamic organelles: peroxisome abundance in yeast. FEBS J. 277, 3279–3288.
Shiba, Y., Paradise, E.M., Kirby, J., Ro, D.K., Keasing, J.D., 2007. Engineering of the pyruvate dehydrogenase bypass in *Saccharomyces cerevisiae* for high-level production of isoprenoids. Metab. Eng. 9, 160–168.
Spanova, M., Czabany, T., Zellnig, G., Leitner, E., Hapala, I., Daum, G., 2010. Effect of lipid particle biogenesis on the subcellular distribution of squalene in the yeast *Saccharomyces cerevisiae*. J. Biol. Chem. 285, 6127–6133.
Ta, M.T., Kapterian, T.S., Fei, W.H., Du, X.M., Brown, A.J., Dawes, I.W., Yang, H.Y., 2012. Accumulation of squalene is associated with the clustering of lipid droplets. FEBS J. 279, 4231–4244.
Tetali, S.D., 2019. Terpenes and isoprenoids: a wealth of compounds for global use. Planta 249, 1–8.
van Roermund, C.W.T., Drissen, R., van den Berg, M., Ijlst, L., Hettema, E.H., Tabak, H.F., Waterham, H.R., Wanders, R.J.A., 2001. Identification of a peroxisomal ATP carrier required for medium-chain fatty acid beta-oxidation and normal peroxisome proliferation in *Saccharomyces cerevisiae*. Mol. Cell. Biol. 21, 4321–4329.
Voth, W.P., Richards, J.D., Shaw, J.M., Stillman, D.J., 2001. Yeast vectors for integration at the HO locus. Nucleic Acids Res. 29.
Walsh, C., 2000. Molecular mechanisms that confer antibacterial drug resistance. Nature

406, 775–781.
Wei, L.J., Kwak, S., Liu, J.J., Lane, S., Hua, Q., Kweon, D.H., Jin, Y.S., 2018. Improved squalene production through increasing lipid contents in *Saccharomyces cerevisiae*. Biotechnol. Bioeng. 115, 1793–1800.
Westfall, P.J., Pitera, D.J., Lenihan, J.R., Eng, D., Woolard, F.X., Regentin, R., Horning, T., Tsuruta, H., Melis, D.J., Owens, A., Fickes, S., Diola, D., Benjamin, K.R., Keasling, J.D., Leavell, M.D., McPhee, D.J., Renninger, N.S., Newman, J.D., Paddon, C.J., 2012. Production of amorphadiene in yeast, and its conversion to dihydroartemisinic acid, precursor to the antimalarial agent artemisinin. Proc. Natl. Acad. Sci. U.S.A. 109, 111–118.
Xie, W.P., Lv, X.M., Ye, L.D., Zhou, P.P., Yu, H.W., 2015a. Construction of lycopene-overproducing Saccharomyces cerevisiae by combining directed evolution and metabolic engineering. Metab. Eng. 30, 69–78.
Xie, W.P., Ye, L.D., Lv, X.M., Xu, H.M., Yu, H.W., 2015b. Sequential control of biosynthetic pathways for balanced utilization of metabolic intermediates in *Saccharomyces cerevisiae*. Metab. Eng. 28, 8–18.
Xie, Z.X., Mitchell, L.A., Liu, H.M., Li, B.Z., Liu, D., Agmon, N., Wu, Y., Li, X., Zhou, X., Li, B., Xiao, W.H., Ding, M.Z., Wang, Y., Yuan, Y.J., Boeke, J.D., 2018. Rapid and efficient CRISPR/Cas9-Based mating-type switching of *Saccharomyces cerevisiae*. G3-Genes Genom Genet. 8, 173–183.
Yablon, D.G., Schilowitz, A.M., 2004. Solvatochromism of nile red in nonpolar solvents. Appl. Spectrosc. 58, 843–847.
Yao, Z., Zhou, P.P., Su, B.M., Su, S.S., Ye, L.D., Yu, H.W., 2018. Enhanced isoprene production by reconstruction of metabolic balance between strengthened precursor supply and improved isoprene synthase in *Saccharomyces cerevisiae*. ACS Synth. Biol. 7, 2308–2316.
Ye, L.D., Lv, X.M., Yu, H.W., 2016. Engineering microbes for isoprene production. Metab. Eng. 38, 125–138.
Yee, D.A., DeNicola, A.B., Billingsley, J.M., Creso, J.G., Subrahmanyam, V., Tang, Y., 2019. Engineered mitochondrial production of monoterpenes in *Saccharomyces cerevisiae*. Metab. Eng. 55, 76–84.
Yuan, J.F., Ching, C.B., 2016. Mitochondrial acetyl-CoA utilization pathway for terpenoid productions. Metab. Eng. 38, 303–309.
Yuan, W., Veenhuis, M., van der Klei, I.J., 2016. The birth of yeast peroxisomes. Bba-Mol Cell Res. 1863, 902–910.
Zhang, C.B., Liu, J.J., Zhao, F.L., Lu, C.Z., Zhao, G.R., Lu, W.Y., 2018. Production of sesquiterpenoid zerumbone from metabolic engineered *Saccharomyces cerevisiae*. Metab. Eng. 49, 28–35.
Zhao, C., Kim, Y., Zeng, Y.N., Li, M., Wang, X., Hu, C., Gorman, C., Dai, S.Y., Ding, S.Y., Yuan, J.S., 2018. Co-compartmentation of terpene biosynthesis and storage via synthetic droplet. ACS Synth. Biol. 7, 774–781.
Zhao, J., Li, C., Zhang, Y., Shen, Y., Hou, J., Bao, X., 2017. Dynamic control of ERG20 expression combined with minimized endogenous downstream metabolism contributes to the improvement of geraniol production in *Saccharomyces cerevisiae*. Microb. Cell Factories 16.
Zhou, Y.J., Buijs, N.A., Siewers, V., Nielsen, J., 2014. Fatty acid-derived biofuels and chemicals production in *Saccharomyces cerevisiae*. Front. Bioeng. Biotechnol. 2 32-32.